MODELLING OF WAVE TRANSMISSION THROUGH POROUS VERTICAL COASTAL STRUCTURES

by

S. S. L Hettiarachchi

1.0 Introduction and Objective of the study

The wave field in the vicinity of a coastal structure may be treated in terms of dissipated, reflected and transmitted components. The transmitted energy has two components, transmission by overtopping and transmission through the structure, the latter being applicable to porous structures.

Most wave energy dissipating structures are designed having some degree of porosity, the presence of which increases the energy dissipation characteristics of the structure. There are also a certain category of structures which are permeable in that they permit, to a high degree, wave transmission into the structure. In this context porous coastal structures designed to dissipate wave energy may be broadly classified under two categories, namely, armoured porous slopes and porous vertical walls.

The advantages of vertical face structures over those with sloping faces lie in the efficient use of space, economy of material and the ability to moor vessels along side, factors which are of considerable importance to coastal and harbour engineers. Problems arising due to wave reflections from solid vertical faces suggest a number of alternative forms of construction of which one approach is to form a vertical face structure which itself includes sufficient porosity, in an appropriate configuration, so as to allow significant energy dissipation within the body of the structure. Porous vertical structures must dissipate wave energy in a gradual manner to avoid undue reflections and significant energy absorption will require a structure of reasonable horizontal dimension in relation to the incident wave length. Examples of types of structures which can be classified under this category include

a) gabion walls or cribwork

b) stacked voided blockwork

c) perforated caissons

d) piled wave screens

The objective of this paper is to present the results of an investigation on wave transmission through porous vertical structures. The first part refers to the development of a numerical model for unsteady, one-dimensional non-Darcy flow through porous structures, for the prediction of transmission characteristics within the structure. The second part refers to an experimental study to measure wave transmission through a porous absorber consisting of stacked voided concrete blocks and to measure interface losses at the wave-structure interface. The third part refers to the evaluation of the model and its applications.

Several researchers have investigated the interaction of water waves with porous coastal structures. The mathematical treatment of the subject has only been possible under several simplifying assumptions which are reasonably justified in view of the complex nature of the problem. Some of the assumptions have been necessary due to the absence of quantitative expressions to identify and describe certain complex interactions between wave motion and porous coastal structures. Both analytical and numerical techniques have been used to model wave action on different types of coastal structures. Hall and Hettiarachchi (1991) review the mathematical modelling of wave action on coastal structures and attention is focused on the formulation of the governing equations and the solution techniques.

2.0 Numerical Developments

2.1 Governing equations

The phenomenon to be modelled is shown in Figure 1. The governing equations for horizontal momentum

Eng.(Dr) S S L Hettiarachchi - BSc Eng, PhD,(Lond), DIC
Senior Lecturer, Department of Civil Engineering
University of Moratuwa.

and continuity for flow inside the structure and the total differentials for u and h are expressed as,

$$\frac{u}{n}\frac{\partial u}{\partial x} + \frac{\partial u}{\partial t} + gn\frac{\partial \eta}{\partial x} = -gnfu \qquad (1)$$

$$\left[\frac{ho+\eta}{n}\right]\frac{\partial u}{\partial x} + \frac{u}{n}\frac{\partial \eta}{\partial x} + \frac{\partial \eta}{\partial t} = 0 \qquad (2)$$

$$du = \frac{\partial u}{\partial x}dx + \frac{\partial u}{\partial t}dt \qquad (3)$$

$$d\eta = \frac{\partial \eta}{\partial x}dx + \frac{\partial \eta}{\partial t}dt \qquad (4)$$

where

- u is the depth averaged horizontal velocity (discharge velocity)
- h is the free surface elevation with respect to the still water level
- n is the porosity

The Forchheimer equation is used to estimate the non-Darcy term:

$$F = a + b[u] \qquad (5)$$

This arises from the hydraulic gradient velocity relationship

$$I = au + bu^2 \qquad (6)$$

where a and b are laminar and turbulent steady flow coefficients.

At this stage it is convenient to make the dependent variables u and h dimensionally identical through the transformation,

$$c = \sqrt{g(h_0+\eta)} \qquad (7)$$

where c represents wave celerity as obtained from the long wave approximation.

The equations of motion and continuity can now be expressed in terms of u and c as follows.

$$\frac{\partial u}{\partial t} + \frac{u}{n}\frac{\partial u}{\partial x} + 2cn\frac{\partial c}{\partial x} = -gnFU \qquad (8)$$

$$2\frac{\partial c}{\partial t} + \frac{c}{n}\frac{\partial u}{\partial x} + 2\frac{u}{n}\frac{\partial c}{\partial x} = 0 \qquad (9)$$

2.2 Finite difference formulation and the method of solution

Of the several methods available for the numerical solution of the above set of equations, a finite difference scheme was adopted. In using finite difference methods the objective is to solve the equations of motion and continuity for unsteady one dimensional non-Darcy flow at a finite number of grid points in the (x,t) plane.

Although the conservation of mass and momentum for any confined velocity field may be represented by a set of partial differential equations, these equations can be written in many finite difference forms using either an explicit or implicit scheme.

This paper considers wave decay within a porous structure and it is intended to study this decay at close intervals in order to monitor the wave propagation. For this purpose small values of have to be chosen. In general, implicit methods result in higher computational cost per grid point per time step and it would be more economical to use an explicit method for this study. It should be noted that stability plays a decisive role with regard to explicit methods and it is important to ensure that the stability criteria are met without undue restrictions on Δt and Δx.

An explicit scheme with central differences in space and forward differences in time is used to discretize eqs. 8 and 9. In finite difference form the equations are expressed as,

$$u(i,j+i) = u(i,j) - \frac{\Delta t}{2\Delta x}\left[\frac{u(i,j)}{n}[u(i+1,j) - u(i\text{-}j)] + 2nc(i\,j)\,c(i+j) - c(i-1,j) + gn\,2\Delta x F(i,j)\right] \qquad (10)$$

$$c(i,j+i) = c(i,j) - \frac{\Delta t}{2\Delta xn} \left[u(i,j) \quad [\,(ci+1,j) \; - \; \frac{c\,(i-1,j)}{2} \; + \; [\,u\,(i+1,j) - u\,(i\text{-}1,j)\,] \right] \tag{11}$$

The critical $\Delta t \,/\, \Delta x$ ratio that should ensure convergence and stability at all times is based on the maximum possible values of u and c and generalized over the entire solution domain. Eqs. 10 and 11 are then solved to advance the values of u and c at all the mesh points , exclusive of boundaries, from the initially still water level. Boundary conditions are then incorporated in order to obtain the complete solution.

2.3 Boundary conditions

With reference to Figure 1 the right hand boundary condition indicates a zero normal velocity at the impervious vertical boundary. The left hand boundary condition represents the experimentally-determined movement of the outcrop point.

The left hand boundary (open boundary) which represents the prescribed time dependent movement of the outcrop point relative to the external wave may require special attention under certain conditions. When water enters the porous medium (during the rising stage), the outcrop point, C, in Figure 1 coincides approximately with the free, external water level. However, the inside and outside water levels may or may not coincide at the interface when the water is flowing out from the porous media. For the latter case a seepage face will be formed. This phenomena has been observed for materials such as crushed rock having a comparatively low value of porosity. Low permeability of the porous medium facilitates the development of a seepage face. This concept was analysed in detail by Dracos (1969) for Darcy flow and based on this analysis Nasser (1977) recommended a numerical procedure to be included in the modelling of non-Darcy flows. However, the effectiveness of this phenomenon for various types of porous media has not been subjected to detailed investigation. For the experimental results discussed in this paper it was observed that for media with a relatively high value of porosity, the outcrop point coincides with the free water level. Small wave amplitudes and a uniform distribution of the voids in all three dimensions favour this coincident water level condition.

For this situation the following boundary conditions will be used

(i) The right hand boundary condition at the impervious boundary is u = 0 for all values of t.

(ii) The left hand boundary condition is a sine function representing the external wave assuming that the outcrop point coincides with the free water level.

From the foregoing discussion it is evident that only one of the two dependent variables (u and c) is known at each boundary. Although the discretized equations of motion and continuity (eqs. 10 & 11) may be used to evaluate the unknown variables, this does not make use of all the information available. A refined approximation is adopted in which the unknown dependent variable at one boundary is evaluated by incorporating the other dependent variable, known at time (j +1). This is easily achieved by a combination of the momentum and continuity equations.

Subtracting the continuity equation from the momentum equation and using a forward finite difference scheme yields the left hand boundary condition at i=1.

Adding the continuity and momentum equations and using a forward finite difference scheme yields the right hand boundary condition at i=N, in which u=0 is substituted for all t at i=N.

2.4 Initial conditions

The external wave input at the left hand boundary (open boundary) is expressed as a sine function of the form

$$\eta = A_0 \sin 2\pi \frac{t}{T} \tag{12}$$

Where

A_0 is the amplitude of the input wave

T is the period of the input wave

Wave celerity is given by

$$c = \sqrt{g\,(h_0 + \eta)} \tag{7}$$

and in more general form as applicable to the model

$$c\,(1, j+1) = \sqrt{g\,(h_0 + A_0 \sin \frac{2\pi\,(j)\,\Delta t}{T}} \tag{13}$$

for all j, is used for the program.

Initial conditions for the problem are as follows,

u = 0 and h = 0 at all grid points at the start of the time interval (at t = 0).

$\eta = 0$ yields that $c\,(i,1) = \sqrt{gh_0}$ (14)

$u = 0$ results in $u\,(i,1) = \sqrt{0}$ (15)

In computing the u(i,j+1) term, the friction term is evaluated from u(i,j) i.e. F(i,j). However, it would be more appropriate if this is based on the values of velocity corresponding to both (i,j+1) and (i,j). In the numerical scheme adopted an iterative procedure is employed to adjust the non-linear friction term, F, velocities u and celerities, c, at all mesh points by averaging the values between two successive time increments until a specific tolerance is reached. The iteration was carried out for five cycles and it was observed that the solution converges and only a difference in the fourth decimal place was observed when comparing with the original values.

The input wave amplitude , of the numerical model corresponds to the movement of the outcrop point which is considered to coincide with the free water level for wave absorbers having a high three dimensional porosity, an assumption proved valid from experimental observations of this study. Hence , in eq. 12 refers to water level fluctuation at the interface and not the anti-node heights (Hmax) observed further away in experimental measurements, although they may be approximately equal. When using this parameter for computation it is also important to include the effect of interface losses which will be discussed later.

2.5 Properties of the finite difference scheme

Approximation, truncation error, consistency, discretization error, convergence, stability and accuracy are the important numerical properties of any finite difference scheme and these should be given due consideration in developing an acceptable predictive model. Attention should be focused on the conditions that must be satisfied if the solution of the finite difference equation is to be a sufficiently accurate approximation to the solution of the partial differential equation.

The finite difference scheme adopted in this study satisfies the requirement of being unconditionally consistent with the original equations. Thus, from the standpoint of consistency, the finite difference scheme adopted represent the governing equations without any residual terms arising through the truncation errors.

Although a difference scheme may be consistent with the corresponding differential equations, the solution to the former need not necessarily converge to that of the latter as . It is possible , for certain values of the time step and the grid size , that the numerical solution will either become unstable or may even converge to an incorrect analytical solution.

It is difficult to develop directly convergence conditions for the governing equation used in the study. Procedures have been developed to investigate convergence through stability and consistence conditions. Use is made of the Equivalence theorem which states that if the difference scheme is stable and consistent with the differential equation then its solution will converge to that of the differential equation.

For analytical investigations of the stability of finite difference schemes, one of the two standard methods can be used (Smith 1979). The first method involves expressing the equations of motion in matrix form and examining the eigen values of the associated amplification matrix. In the second method, the eigen values are determined by using a finite Fourier series and this method was used to test the stability of the model.

To determine the influence of the non-linear terms on the stability of a finite difference scheme, it is not correct to consider the propagation of one Fourier component as in the case of a linear set of difference equations. This is because different components of the Fourier series will interact with one another through the non-linear terms. However, it is possible to investigate the stability of a non-linear difference scheme by considering a linearised version of the equation. This is achieved by resolving the non-linear terms into linear components with constant coefficients (Liggett and Cunge 1975). By considering the corresponding quasi-linearised momentum and continuity equations, the general stability condition was found to be

$$\Delta t \leq \frac{gFn}{\left[\frac{gfn}{2}\right] + \left[\frac{c_0 + upo}{\Delta x}\right] \sigma in2\,(s\Delta x)} \qquad (16)$$

in which the new parameters are

$$\sigma = \frac{2\pi}{L} \quad \text{and} \quad = \frac{u_p}{n}$$

2.6 Internal transmission coefficients

Wave attenuation inside the structure is studied by identifying an internal transmission coefficient. This coefficient which varies with location along the length of the structure, is defined at any given point , by

$$K_t = \frac{H_x}{{}_{tx}H_0} \qquad (17)$$

where

- H_x is the measured wave height within the structure at a distance x from the front interface
- H_0 is the loop height at the front interface obtained from experiments
- l is the length of the structure

In applying the model to experimental data, it is necessary to account for interface losses which could be accommodated by introducing the expression for, the transmission coefficient at the front interface. Therefore eq. 17 can be expressed as

$$K_t = \frac{H_{tf}}{H_0} \cdot \frac{H_x}{H_{tf}} \tag{18}$$

where

H_{tf} is the wave height transmitted at the front interface

$$K_{tf} = \frac{H_{tf}}{H_0} \tag{19}$$

is the transmission coefficient at the front interface.

Results from experiments on interface losses were used to estimate the ratio $\frac{H_{tf}}{H_0}$ in eq. 18. If this term is not included the predicted transmission coefficients will be comparatively higher than those observed in the experiments with the model over-predicting wave transmission.

2.7 Input parameters for the model

The model input parameters are the laminar and turbulent steady flow coefficients (a and b) in the Forchheimer equation, porosity (n), length of structure (l), still water depth (h_0), wave period (T) and the incident wave amplitude, which is represented in the form of the movement of the outcrop point. The interface losses are accommodated via a transmission coefficient for the front interface, determined experimentally.

3.0 Experimental investigations

In order to evaluate the numerical model, experimental data were obtained by conducting a series of two dimensional model tests using regular waves on two vertical face porous absorbers having an impermeable face at the back. The loop- node technique was used to identify the incident and reflected wave heights. The internal wave transmission was measured at regular intervals along the structure by using a wave probe. The absorbers of length 160 cm were assembled by using model Cob and Shed armour units (Figure 2). The overall porosity of the structure was of the order of 62%.

In order to determine the laminar and turbulent flow coefficients a and b in the Forchheimer equation, a series of tests were carried out on block of Cob and Shed units under steady flow conditions. Here again rectangular blocks consisting of Cob and Shed units were placed in a flume and the head loss across the structure was measured under steady flow conditions for varying discharges. Thus the coefficients a and b obtained in the experimental programme under steady, free flow conditions seems more appropriate for the mathematical simulation than that of values obtained by closed permeameters.

It is identified that in most laboratory flumes, the distance from the wave generator to the model is of limited length and the incident wave height cannot be measured without being disturbed by the influence of the reflected wave. With regard to vertical porous structures the composite wave generated in front of the structure by the action of regular waves consists of a partial standing wave. With reference to this wave system it is noted that in laboratory experiments the wave height at the open boundary will not correspond to the height of the anti-node observed further away from the structure. Surface distortions occur in the immediate vicinity of the structure due to run-up and run-down on the vertical permeable interface. The problem is further complicated by interface losses which reduces the wave height across the front interface and by the possible effect of air entrainment.

An estimate of the interface losses is best obtained by performing a series of wave transmission /reflection tests on a structure of negligible length but representing accurately the fluid structure interface. Since these losses are closely related to the two-dimensional porosity of the interface it is important to perform tests on the accurately reproduced interface having negligible length in the direction of wave propagation. To perform these tests on randomly packed porous media is difficult because of the practical limitations associated in creating the structural configuration required for the experiment. However this is easily achieved in the case of rectangular porous structures consisting of model Cob and Shed armour units. Since these units are produced in two equal halves pinned together, it is possible to assemble a vertical screen which produces the interface accurately while limiting the length (in the direction of wave propagation) to less than 20 mm.

The results from the experiments showed that the transmission coefficients for the two vertical screens lie between 0.65 and 0.85 which is quite low when considering the two dimensional porosity (20%-23%) and the very short length of the structure. The transmission coefficients decease with increasing steepness and from the analysis of experimental results it was found that in the range , $0.010 < \frac{H_i}{L} < 0.035$, K_{tf} can be expressed as,

$$K_{if} = -8.712 \frac{H_i}{L} + 0.909 \tag{20}$$

This result was incorporated in the numerical model to account for interface losses.

4.0 Evaluation of the theoretical analyses

4.1 Comparison with experimental data

Results from the application of the numerical model to the absorber are presented in Figures 3 to 6. These plots refer to wave periods of 1.0, 1.5 and 2.0 secs at a mean depth of 23 cm. Figures 3 and 4 refer to wave period 2.0 secs but with different incident wave heights. In applying the model, interface losses were accommodated by introducing in eq. 18 the expression for given by eq. 20. It is evident that the agreement between experimental and predicted results are very satisfactory.

The restriction of the ratio between time and space increments imposed by eq. 16 produced solutions satisfying conditions for numerical convergence and stability. The influence of the grid size used in discretizing the x-t plane was investigated by applying the model for the 160 cm long absorber with values of ranging from 16 to 40 cm. The finer grid produced better agreement and the results presented refer to the 16 cm grid size.

4.2 Sensitivity analysis

Apart from the verification of the numerical model by comparison with experimental data, certain features of the model in relation to its applicability for different porous structures and varying conditions were also investigated. This was achieved by studying the response of the model output to variation in key parameters. For this purpose three approaches were adopted. Modifications for interface losses were not included in the analysis.

In the first approach the model was applied to investigate the flow through five rectangular absorbers each of length 150 cm, consisting of model Cob units, model Shed units and cylindrical lattice structures of 15, 20 and 30 mm diameter. In each case it was assumed that the structure was located at a water depth of 38 cm and subjected to waves of period 2.0 secs and an incident wave amplitude of 18 cm at the front interface. The laminar and turbulent flow coefficients were obtained for the experimental media by conducting steady flow permeability tests. The results from this exercise are given in Table 1 and represent the variation of internal transmission coefficients given by eq. 17 versus distance along the length of the structure.

This table clearly illustrates that as the turbulent flow coefficient increases, the wave amplitude decreases more rapidly as the wave propagates within the structure. This observation is consistent with the physics of flow through porous media. In this context it should be noted that under steady flow conditions, the hydraulic gradient was expressed by the Forchheimer relationship (eq. 6) from which it is evident that for , $I_{turbulent} > I_{laminar}$, the macroscopic velocity „ should satisfy u a/b respectively. For the incident wave system adopted in this study, the horizontal orbital velocity at the free surface corresponding to wave heights at the front and rear interfaces are approximately equal to 1.00 and 0.35 m/sec respectively. The values of the critical velocity $u_c = a/b$ for different media are also given in Table 1 and it was seen that the minimum orbital velocity exceeds the critical value for three of the structures. This gives an indication of the degree of turbulence associated with the respective structures and the importance of the turbulent term in relation to energy dissipation. If interface losses were included in the analysis it would have increased the damping characteristics of the media, particularly for the absorbers consisting of Shed and Cob armour units.

The second approach examined the sensitivity of the flow coefficients by analysing the response of the solution to an increment (+ 25%) in both laminar and turbulent flow coefficients. This study was limited to the absorber consisting of model Shed armour units used in the first experiment. The results from this exercise are presented in Table 2 and indicate the percentage variation in the wave height along the length of structure due to positive and negative increments in a and b. The results illustrate the greater influence of the turbulent flow coefficient (b) on the damping characteristics of the wave absorber.

The third approach examined the sensitivity in relation to variation with wave period. This study was also limited to the absorber consisting of model Shed armour units but under a different wave environment to that of the previous two cases. The structure was of length 150 cm but was in still water depth of 20 cm and subjected to waves having an amplitude of 5.0 cm at the front interface. Five wave periods 1.0, 2.0, 3.0 4.0 and 5.0 secs were used for the experiment. The results from this experiment are presented in Table 3 and represent the variation of the internal transmission coefficient defined by eq. 17 along the length of the structure. The results illustrate that waves having a higher period are more effectively transmitted through the structure in comparison with those having a lower period.

5.0 Concluding remarks

This paper has presented the results of an investigation on wave transmission through porous vertical structures. A numerical model for the simulation of unsteady, one-dimensional, non-Darcy flow through porous vertical structures has been presented. The models predicts the wave transmission characteristics within the structure. Interface losses at the front interface has been accommodated by the inclusion of a transmission coefficient which is determined by experimental investigations.

The model is evaluated by comparing numerical results with experiment data on stacked voided blockwork consisting of Shed and Cob armour units. The agreement between experimental and predicted results are very satisfactory. The results of a sensitivity analysis to study the response of the model output to variations in key input parameters are also presented. The model has applications in the design of porous vertical structures using stacked voided blockwork for harbour and coastal works.

Stacked voided blockwork have been used widely in the construction of harbours structures, particularly in Japan. The Shed and Cob armour units used in this study have been used successfully as single layer armour blocks in the construction of sloping breakwaters. This study clearly identifies its potential to be used as porous blocks in stacked voided vertical structures. The high porosity of the structure will certainly reduce costs. Certain practical modifications will be required to achieve structural and geotechnical stability of the overall structure. The level of turbulence within the porous structure would be sufficiently high to prevent problems relating to sedimentation. These aspects along with other considerations such as mooring forces have to be considered in the detailed design of the structure.

6.0 References

Dracos, T. (1969) Calculation of the movement of the outcrop point. Proc. XIII, Congress of the IAHR, paper D-2, Kyoto, Japan.

Hall, K.R. and Hettiarachchi, S.S.L. (1991) Mathematical modelling of wave interaction with rubble mound breakwaters. Proc. of Conf. on Coastal Structures and breakwaters, ICE, Thomas Telford, London.

Ligget, J.A. and Cunge, J.A. (1975) Numerical methods of solution of the unsteady flow equations. Chapter 4 of Unsteady flow in open channels. (Ed. Mahmood, K. and Yevjevich, V) Water Resources Publications, Fort Collins.

Nasser, M.S. (1977) The outcrop point movement in non-Darcy flow. Proc. 6th Canadian Congress of Applied Mechanics, Vancouver, Canada.

Smith, G.D. (1979) Numerical solution of partial differential equations. Oxford University Press, London, 2nd Edition.

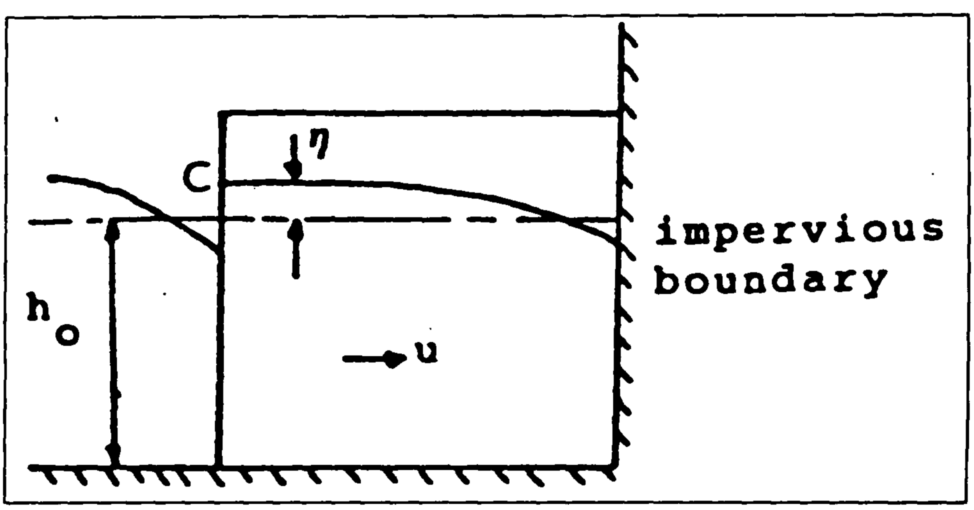

Figure 1 - Structural Configuration used for analyses

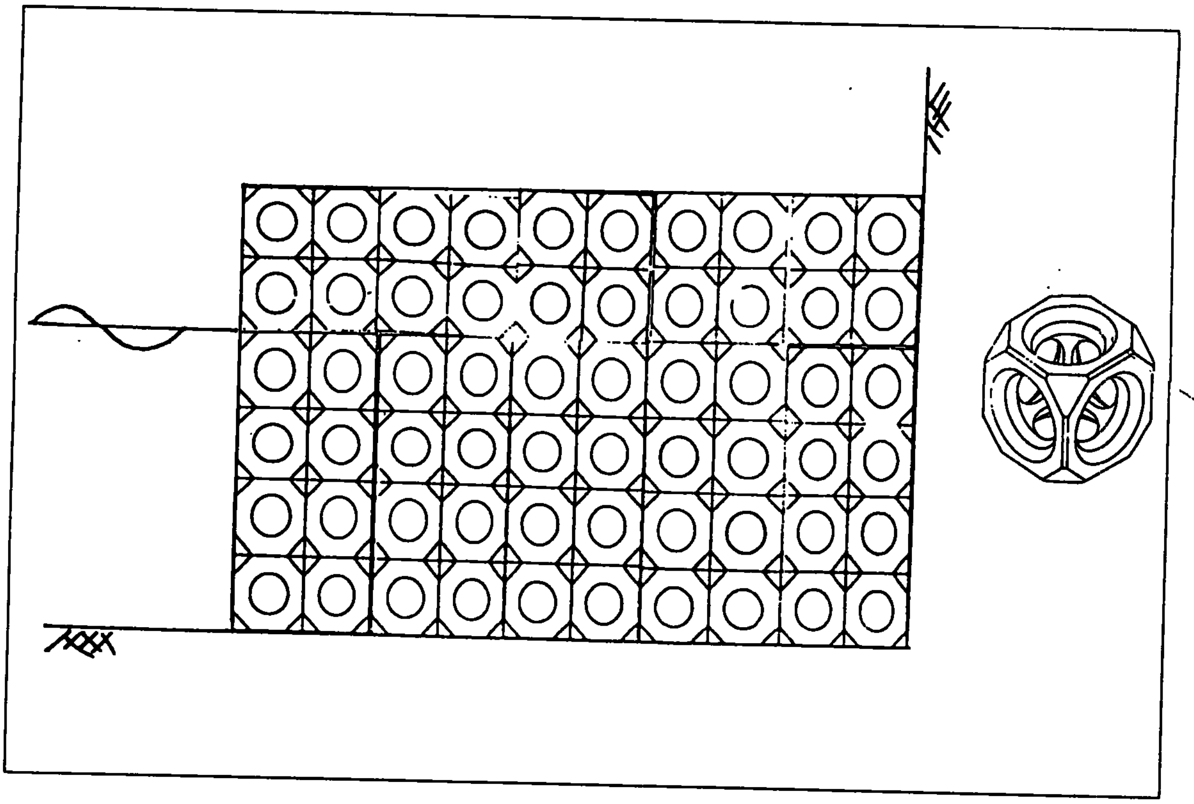

Figure 2 - Porous Wave Absorber Consisting of shed armour units

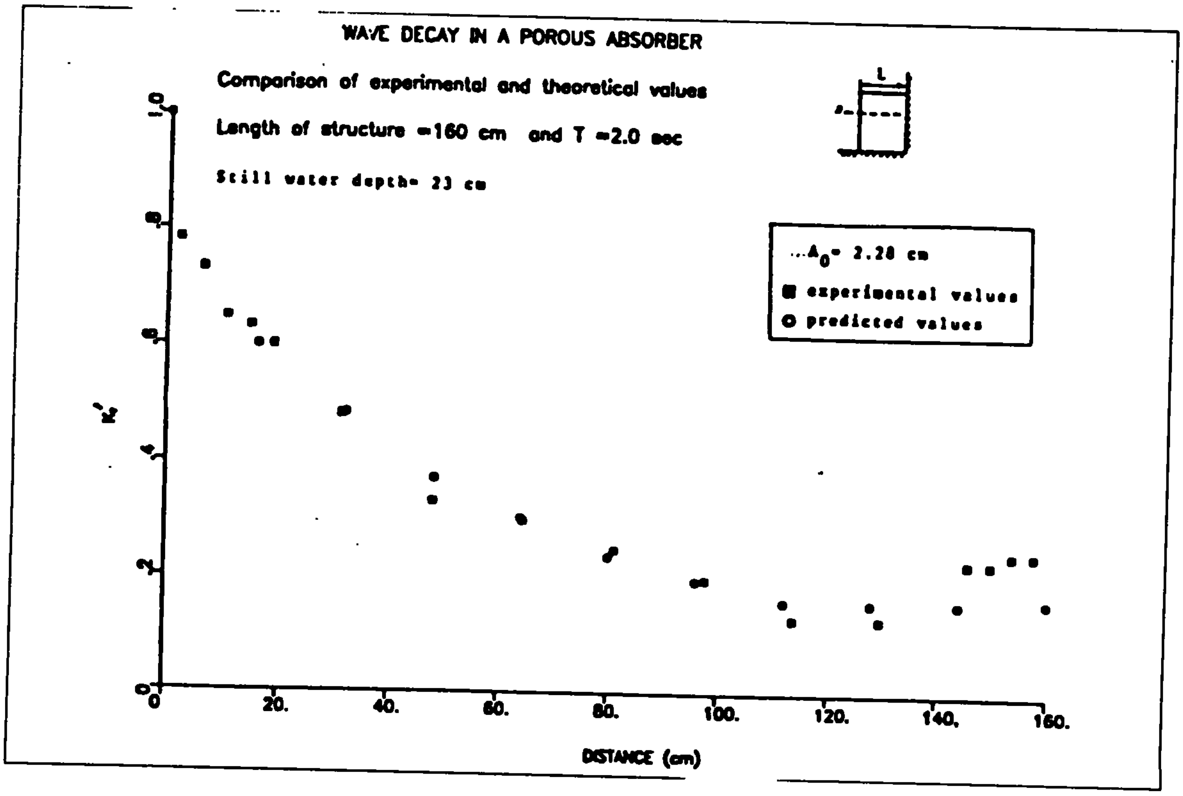

Figure 3 - Wave Decay in a Porous Absorber Comparision of Experimental and Theoretical Values

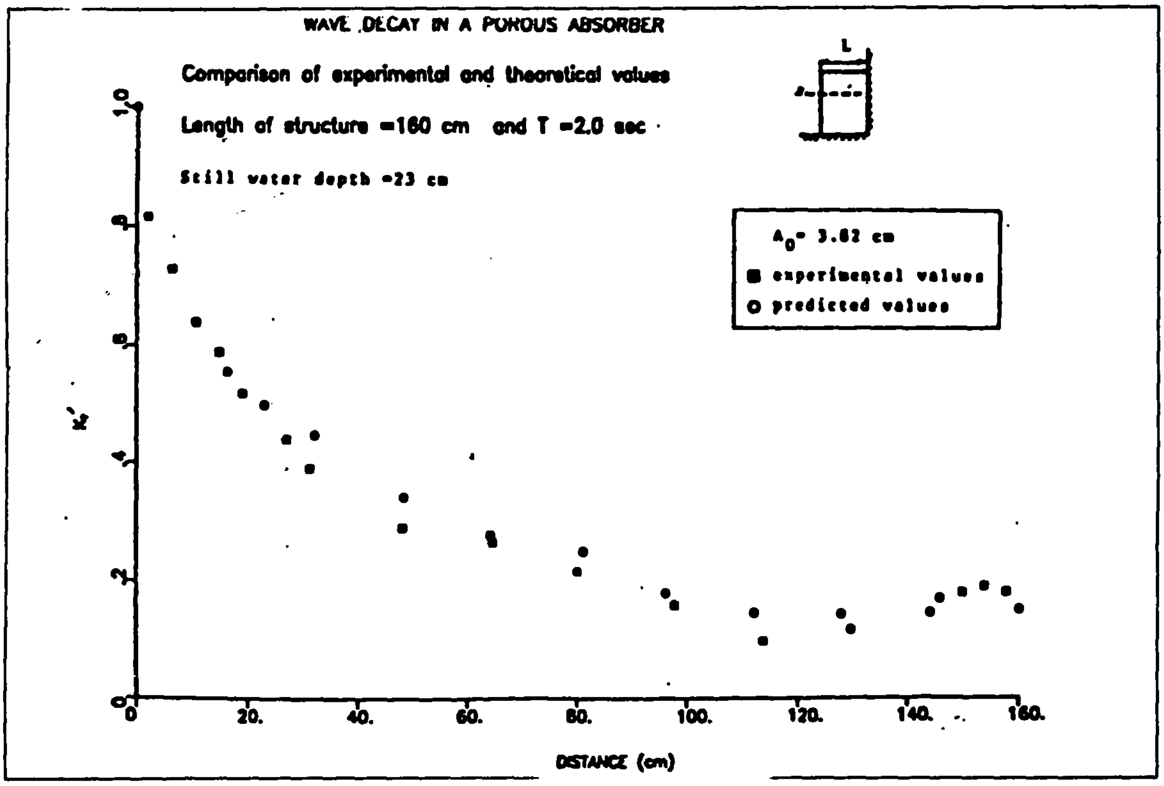

Figure 4 - Wave Decay in a Porous Absorber Comparision of Experimental and Theoretical Values

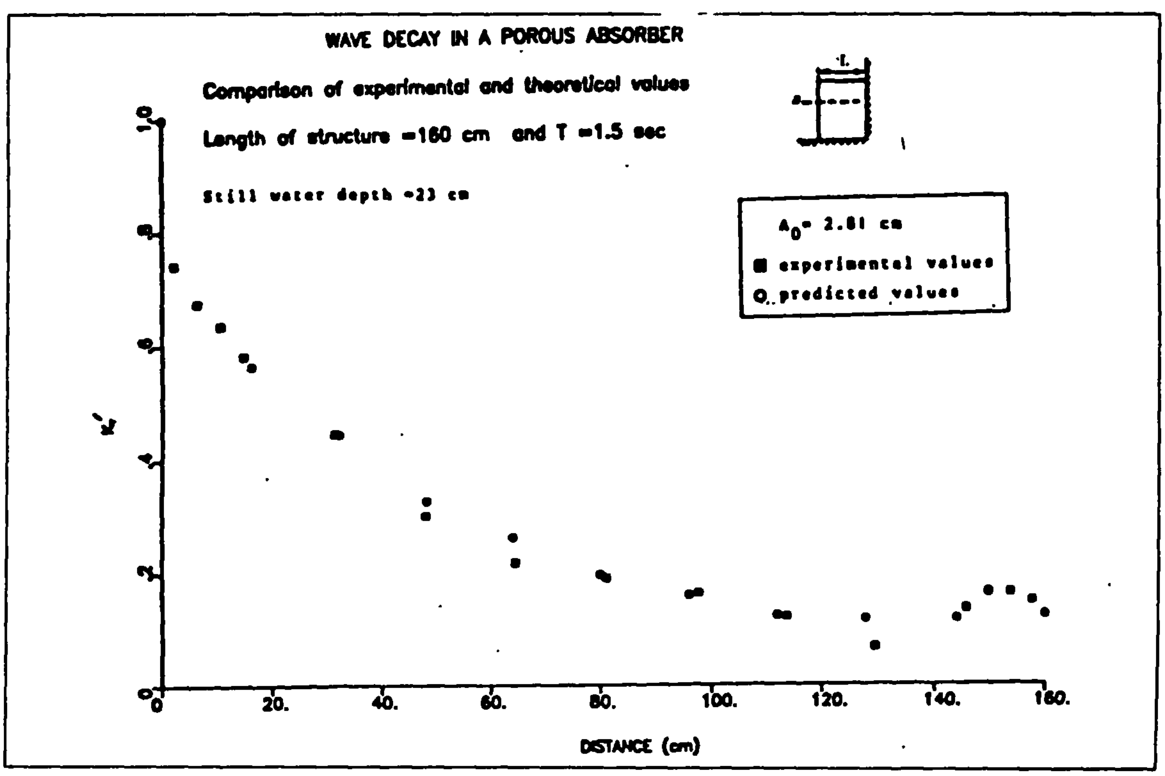

Figure 5 - Wave Decay in a Porous Absorber Comparision of Experimental and Theoretical Values

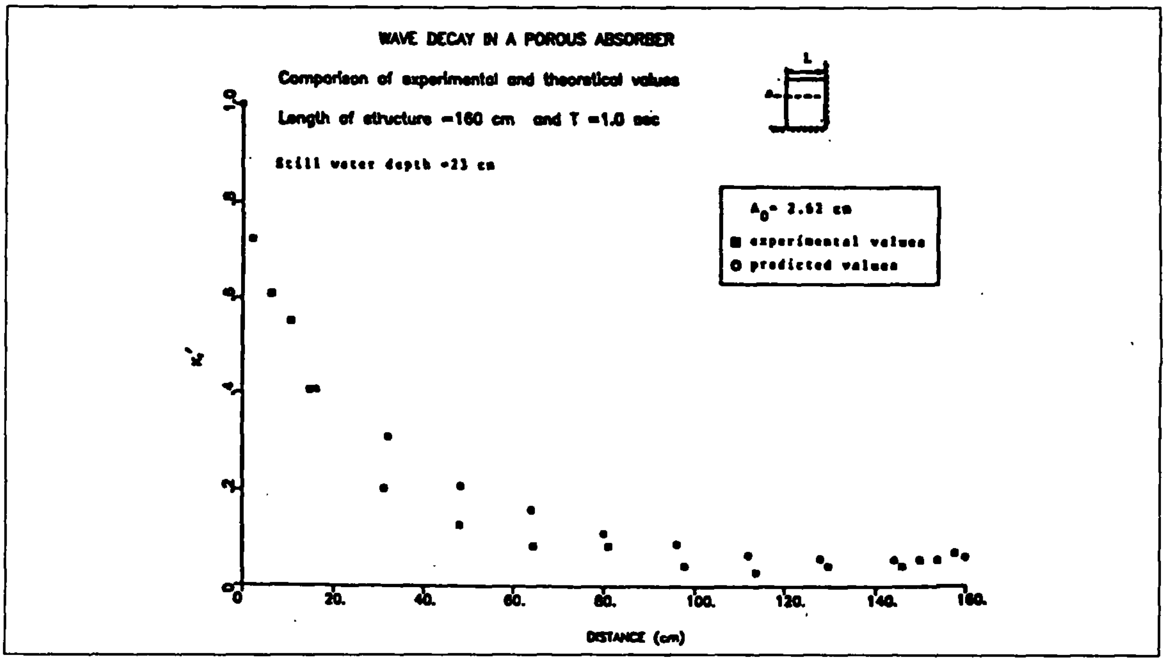

Figure 6 - Wave Decay in a Porous Absorber Comparision of Experimental and Theoretical Values

Table 1

Numerical Solution For The Internal Transmission Coefficients For different Porous Media

	Porous blocks consisting of hollow block armour		cylindrical lattice structures		
	cob	Shed	D=15 mm	D=20 mm	D=30 mm
In I = au + bu²					
a (sec / m)	0.917	0.703	0.612	0.682	0.642
b (sec /m)²	6.407	5.802	3.051	1.338	0.751
u' = a/b (m/sec)	0.143	0.121	0.200	0.510	0.855
n (porosity)	0.627	0.614	0.607	0.607	0.607
Distance along the lenght of structure (cm)	Internal transmission coefficients				
0.0	1.000	1.000	1.000	1.000	1.000
15.0	0.780	0.798	0.850	0.861	0.875
30.0	0.665	0.665	0.745	0.757	0.779
45.0	0.509	0.543	0.641	0.656	0.690
60.0	0.421	0.458	0.564	0.581	0.625
75.0	0.344	0.382	0.475	0.508	0.559
90.0	0.298	0.339	0.452	0.458	0.509
105.0	0.271	0.321	0.470	0.472	0.540
120.0	0.279	0.340	0.521	0.522	0.595
135.0	0.287	0.353	0.543	0.548	0.632
150.0	0.292	0.359	0.548	0.555	0.647

Incident wave amplitude A_0 = 18 cm
wave period = 2 sec
Still water depth = 38 cm

Numerical Solution for The Internal Transmission coefficients For different Porous Media

Table 2

Response of The Numerical Solution to variations in Lanminar and Turulent flow Coefficients

Rectangular porous absorber consisting of Shed armour units

Distance along the length of structure (cm)	1 a = 0.7034 b = 5.8022 Values obtained from steady flow tests	2 a = 0.7034 b = 7.2528 increase of b by 25%	3 a = 0.8793 b = 5.8022 increase of a by 25%	4 a = 0.7034 b = 4.3517 decrease of b by 25%	5 a = 0.5276 b = 5.8622 decrease of a by 25%
	wave amplitude	- wave amplitude and - Percentage reduction in wave amplitude with respect to values given in column 1 Percentage reduction in wave height = (A - A,) / A1 % A is the wave amplitude A_1 is the corresponding wave amplitude in column 1			
0.0	18.00	18.00	18.00	18.00	18.00
15.0	14.40	14.44 -1.81%	14.26 -0.96%	14.69 +2.03%	14.54 +0.96%
30.0	12.01	11.64 -3.03%	11.79 -1.83%	12.41 +3.39%	12.23 +1.84%
45.0	9.82	9.40 -4.29%	9.54 -2.87%	10.31 +4.98%	10.11 +2.91%
60.0	8.28	7.85 -5.16%	7.96 -3.82%	8.79 +6.19%	8.60 +5.19%
75.0	6.91	6.50 -6.00%	6.57 -4.96%	7.42 +7.32%	7.27 +5.19%
90.0	6.12	5.72 -6.49%	5.72 -6.47%	6.61 -7.96%	6.55 +7.00%
105.0	6.14	5.65 -7.24%	5.50 -9.01%	6.78 +9.22%	6.89 +10.48%
120.0	6.14	5.65 -8.08%	5.50 -10.47%	6.78 +10.45%	6.89 +12.11%
135.0	6.39	5.86 -8.20%	5.68 -11.08%	7.07 +10.60%	7.20 +12.63%
150.0	6.51	6.00 -8.13%	5.79 -11.07%	7.19 +10.44%	7.32 +12.57%

Incident wave amplitude Ao = 18 cm
wave period = 2 sec
Still water depth = 38 cm

Pesponse of The Numerical solution To Variations In laminar and Turbulent Flow Coefficients

Table 3

Sensitivity of The Numerical Solution To Variation In Wave period

Rectangular porous absorber consisting of shed armour units

Distance along the Length of structure (cm)	-Internal transmission coefficients and - Percentage reduction in wave amplitude with respect to the incident wave amplitude (A_0). i. e. 100 (A_0 - Ax) / A_0 for varying periods.				
	T= 1.0 sec	T= 2.0 sec	T=3.0 sec	T=4.0 sec	T= 5.0 sec
0.0	1.0	1.0	1.0	1.0	1.0
15.0	0.633 36.72%	0.758 24.16%	0.802 19.78%	0.830 17.00%	0.848 15.16%
30.0	0.483 51.72%	0.618 38.20%	0.672 32.76%	0.710 28.98%	0.737 26.32%
45.0	0.337 66.34%	0.484 51.64%	0.550 44.98%	0.597 40.30%	0.632 36.76%
60.0	0.264 73.60%	0.399 60.08%	0.466 53.40%	0.517 48.28%	0.561 43.94%
75.0	0.195 80.54%	0.319 68.06%	0.389 61.14%	0.448 55.22%	0.503 49.66%
90.0	0.157 84.26%	0.270 73.04%	0.346 65.40%	0.419 58.12%	0.484 51.62%
105.0	0.121 87.86%	0.230 77.04%	0.322 67.76%	0.404 59.56%	0.474 52.62%
120.0	0.113 88.68%	0.236 76.40%	0.335 66.46%	0.416 58.36%	0.485 51.52%
135.0	0.117 88.26%	0.247 75.26%	0.343 65.74%	0.422 57.82%	0.489 51.12%
150.0	0.126 87.40%	0.256 74.42%	0.349 65.10%	0.427 57.30%	0.493 50.68%

Incident wave amplitude A_0 = 5 cm
Still water depth = 20 cm

Sensitivity of The Numerical Solution To Variations In Wave Period